Modulation of Atlantic salmon miRNome response to sea louse infestation

Valentina Valenzuela-Muñoz[a], Beatriz Novoa[b], Antonio Figueras[b] and Cristian Gallardo-Escárate[a]*

[a]Interdisciplinary Center for Aquaculture Research. Department of Oceanography, University of Concepcion, Barrio Universitario s/n, Concepción, Chile

[b]Institute of Marine Research, Spanish National Research Council (CSIC), Eduardo Cabello 6, Vigo, Spain

Corresponding Author *Dr. C Gallardo-Escárate, Universidad de Concepción, P.O. Box 160-C, Concepción 4030000, Chile (e-mail: crisgallardo@udec.cl)*

Abstract

MicroRNAs are non-coding RNA that plays a crucial role in post-transcriptional regulation and immune system regulation. On other hand, sea lice are prevalent parasites that affect salmon farming, generating different degrees of immune suppression depending on the salmon and sea louse species. *Caligus rogercresseyi* for example, which affects the salmon industry in Chile, decreases Th1 response, macrophage activation, TLR-mediated response and iron regulation in infected fish. In this study, we explore Atlantic salmon miRNome during infestation by *C. rogercresseyi*. Using small RNA sequencing, we annotated 1,718 miRNAs for skin and head kidney from infected Atlantic salmon. The most abundant families identified were mir-10, mir-21, mir-30, mir-181 and let7. Significant differences were found between tissue, with 1,404 annotated miRNA in head kidney and 529 in skin. Differential analysis of transcript expression indicated that at an early stage of infestation miRNA expression was higher in head kidney than in skin tissue, revealing tissue-specific expression patterns. In parallel, miRNA target prediction using 3'UTRs from highly regulated immune-related genes and iron metabolism showed that mir-140-4 and mir-181a-2-5 modulate the expression of TLR22 and *Aminolevulinic acid synthase*, respectively. This study contributes knowledge about the immune response of Atlantic salmon during infestation with sea lice.

Keys words: miRNA, RNA-Seq, Atlantic salmon, *C. rogercresseyi*, gene target prediction.

1. Introduction

Advances in recent years in sequencing technologies have enabled the identification of a large number of untranslated transcripts, termed non-coding RNAs. Although non-coding RNAs do not encode proteins, they do play an important role in key biological processes in vertebrate species (Bartel, 2009; Bushati and Cohen, 2007). Their significance is mainly evidenced in what are termed microRNAs (miRNAs), which are small highly conserved RNA sequences of 21-24 nucleotides (Bartel, 2004) that play a crucial role in post-transcriptional regulation, binding to target mRNAs in 3'UTR and repressing translation to proteins (Bartel, 2004; Bartel, 2009). Some miRNAs display tissue-specific patterns, strongly regulating biological processes like development, growth, cell division, metabolism and apoptosis (Bi et al., 2009; Judice et al., 2016; Lindsay, 2008; Sonkoly et al., 2008).

With respect to immune response, miRNAs play critical roles in the adaptive and innate system, participating in hematopoiesis activation in response to pathogenic microorganisms (Davidson-Moncada et al., 2010; Lu and Liston, 2009; O'Connell et al., 2012). They have also been reported as key components in T cell differentiation, modulating the inflammatory response and activating toll-like receptor pathways in macrophages (Lu and Liston, 2009; O'Connell et al., 2012). For instance, miR-181 is preferentially expressed in B-lymphoid cells in mouse bone marrow, and its ectopic expression in hematopoietic stem/progenitor cells results in an increased fraction of B-lineage cells (Chen et al., 2004). Regarding innate response, the presence of lipopolysaccharide induces the expression of miR-155 and miR146, which in turn inhibits the TLR pathway to avoid excessive inflammatory response (Lu and Liston, 2009; Sonkoly

et al., 2008; Taganov et al., 2006). Several studies have reported host modulation of miRNAs during infection by pathogens. For example, significant changes occur in the miRNA profiles of the crab *Eriocheir sinensis* during infection by the motile bacterium *Spiroplasma eriocheiris* (Ou et al., 2012). Differences have also been observed in miRNA expression levels of the flounder *Paralichthys olivaceus* during infection by the viral hemorrhagic septicemia virus (VHSV) (Najib et al., 2016). A high degree of miRNA regulation associated with innate immune response was observed in the Chinese tongue sole *Cynoglossus semilaevis* infected with the bacteria *Vibrio anguillarum* (Sha et al., 2014).

The Atlantic salmon is an important economic resource for aquaculture endangered by prevalent pathogens that have caused significant economic losses Norway, Chile and Canada. The role of miRNAs is critical to understanding transcriptome modulation in fish biology. The miRNA repertoire of Atlantic salmon has been reported (Andreassen et al., 2013; Barozai, 2012; Bekaert et al., 2013) and is mainly associated with toxicological stressors (Kure et al., 2013). The Chilean aquaculture industry has been severely affected by the sea louse *Caligus rogercresseyi*, which feeds on mucus and blood on the fish epidermis, causing tissue damage and immunosuppression and allowing infection by other prevalent pathogens (Fast, 2014; González and Carvajal, 2003). Recent studies have demonstrated that Atlantic salmon infested with *C. rogercresseyi* have specific immune responses involving TLR pathway signaling, Th1 response and nutritional immunity (Valenzuela-Muñoz et al., 2016). Our goal in this study was to explore the Atlantic salmon miRNome during infestation by *C. rogercresseyi* and identify putative target genes associated with differentially expressed miRNAs, which can represent valuable information for developing therapeutic strategies to control sea lice.

2. Materials and methods

2.1 Experimental design and sample collection

Atlantic salmon (*S. salar*, n = 60) weighing 250 ± 12 g were obtained from the Chaperano Hatchery (Multiexport Food SA) in Cochamo, Chile. All fish were reared in brackish water (15 ppm) until smolting, after which specimens were maintained under a 12:12 h light:dark cycle in single-pass flow-through tanks supplied with ultraviolet-treated salt water. The salmon were fed daily with a commercial diet (Micro 200, EWOS). After initial acclimatization for 15 days, individuals were randomly divided into three tanks with 20 fish per tank (500 L). The salmon were starved at least 24 h prior to any manipulation.

Adult female *C. rogercresseyi* were collected during Atlantic salmon harvesting at a commercial aquaculture farm in Puerto Montt, Chile. After collection, the lice were rinsed and transported in aerated, sterile seawater (8 °C) to the experimental laboratory of the Marine Biological Station, University of Concepción, Dichato, Chile. Their egg strings were then removed and placed in culture buckets supplied with a seawater flow at 12ºC and gentle aeration. The eggs were allowed to hatch and develop until the infectious copepodid stage, at which point they were used to infest fish. The culture was carried out according to Bravo (2010). For infestation, the experimental tanks were placed in darkness without water flow for six hours and with a load of 35 copepodids per fish. During the infestation, fish were supplemented with oxygen. Samples were taken before infestation and at 7 and 14 days post-infestation (dpi). Three to four fish were taken from each tank (ten fish per sampling) and anaesthetized with benzocaine. Head kidney and skin from an infected area (area with sea lice attached) were dissected, fixed in RNA Later (Ambion) and stored at -80ºC.

119

120 *2.2 Illumina sequencing of small RNAs*

121 Head kidney and skin samples from ten adult fish infested with *C. rogercresseyi* were used
122 for small RNA library synthesis. Total RNA was extracted from each individual using the
123 Trizol Reagent (Ambion®) following the manufacturer's instructions. Quantity, purity, and
124 quality of the isolated RNA were measured in the TapeStation 2200 (Agilent Technologies
125 Inc., CA, USA) using RNA ScreenTape (Agilent Technologies Inc., CA, USA) according
126 to the manufacturer's instructions. Samples (n=5) with a RIN over 8.0 were pooled for each
127 tissue and sampling point for library construction. Small RNA libraries were constructed
128 using the TruSeq Small RNA Library Preparation Kit (Illumina®, CA, USA). Three
129 biological replicates from each sample pool were sequenced on the MiSeq (Illumina®)
130 platform using 41 cycles at the Laboratory of Biotechnology and Aquatic Genomics,
131 Interdisciplinary Center for Aquaculture Research (INCAR), University of Concepción,
132 Chile.

133

134 *2.3 miRNAs annotation in Atlantic salmon*

135 Low-quality reads from the Illumina sequencing data, reads with a quality score of less than
136 0.05 on the Phred scale, with a short length, or with three or more ambiguous nucleotides,
137 were strictly removed using CLC Genomics Workbench Software (Version 10.01, CLC
138 Bio, Denmark). Any cleaned sequences matching metazoan mRNA, rRNA, tRNA, snRNA,
139 snoRNA, repeat sequences, or other ncRNAs deposited in the NCBI databases
140 (http://www.ncbi.nlm.nih.gov/), RFam (http://rfam.janelia.org/), or Repbase
141 (http://www.girinst.org/repbase/) were discarded. The remaining transcripts were then
142 counted to generate a single small RNA list. These sequences were aligned against pre-

143 miRNA and mature miRNA (5´ and 3´) sequences listed for *Salmo salar, Danio rerio,*
144 *Cyprinus carpio, Fugu rubripes* comprised in miRBase 21 (Kozomara and Griffiths-Jones,
145 2011, 2014). Putative miRNA sequences were checked for secondary fold-back structure
146 predictions using CLC Genomics Workbench Software with default folding conditions.
147
148 *2.4 RNA-seq analysis of Atlantic salmon during C. rogercresseyi infestation*
149 The miRNAs identified were used as references for RNA-seq analyses through different
150 sample points for each tissue. The RNA-seq settings were a minimum length fraction = 0.6
151 and a minimum similarity fraction (long reads) = 0.5. The expression values were set as
152 transcripts per million (TPM), a modification of reads per kilobase of transcript per million
153 mapped reads (i.e. RPKM), designed to be consistent across samples. More specifically,
154 transcript per-million values were normalized by the total transcript count (instead of by the
155 read count) and average read length. The normalizations allowed for assessing
156 overregulated transcripts among different groups (Wagner et al., 2012). The distance metric
157 was calculated with the Manhattan method, with the mean expression level subtracted in 5-
158 6 rounds of *k*-mean clustering. Finally, a Kal's statistical analysis test was used to compare
159 gene expression levels in terms of $\log_2$ fold-change (P = 0.0005; false discovery rate [FDR]
160 corrected). In order to identify co-expression patterns among miRNAs and mRNAs
161 differentially expressed in Atlantic salmon during *C. rogercresseyi* infestation, Pearson
162 correlation coefficient were estimated for each tissue and plotted using the Corrplot library
163 in R (https://cran.r-project.org/).
164
165 *2.5 Prediction of genes targeted by miRNAs from C. rogercresseyi*

166 Three computational target prediction algorithms were used to predict the genes targeted by
167 miRNAs: PITA (Kertesz et al., 2007), miRanda (John et al., 2004), and STarMir (Rennie et
168 al., 2014). The datasets used were the assembled immune-related and iron modulation gene
169 sequences reported by Valenzuela-Muñoz *et al.* (2016) for Atlantic salmon. STarMir was
170 used to search for miRNA seed matches (nucleotides 2–8 from the 5' end of miRNA) in the
171 3'UTR sequences, and miRanda and PITA were used to match entire miRNA sequences.
172 The STarMir parameters was set at free energy < −15 kcal/mol and a score > 50. The
173 results predicted by the two algorithms were combined, and the overlaps were calculated to
174 identify putative target genes in Atlantic salmon. Finally, *in silico* transcription expression
175 analysis was conducted using five immune-related genes (*TLR12, MMP13, COX2, IFNg,*
176 *CCR3*), three iron transport genes (*haptoglobin, ferritin H, IRP2*), three heme biosynthesis-
177 related genes (*ALAs, HO, BLVr*) and their putative miRNAs identified in the Atlantic
178 salmon miRNome.
179
180 *2.6 Real-time quantification of miRNAs and their putative target genes*
181 Mir-21-2, mir-10b-4-3, let7C-1 were analyzed in combination with *CCR3*, *HO* and *Ferritin*
182 genes to determine the transcription expression of miRNAs and their putative target genes.
183 Briefly, total RNA (including miRNAs and mRNAs) from both tissue types and all
184 sampling points was isolated using TRI Reagent® (InvitrogenTM, Carlsbad, CA, USA),
185 according to the manufacturer's protocol. The purity was determined (A260/A280 ratio)
186 with a Nanodrop ND1000 spectrophotometer (Thermo Fisher Scientific, Copenhagen,
187 Denmark), and the integrity was determined by agarose gel under denaturant conditions.
188 The cDNAs were synthesized for mRNA and miRNA expression analysis using the
189 RevertAid H Minus First Strand cDNA Synthesis Kit (Thermo Scientific, Glen Burnie,

Maryland, USA) and the miScript II RT Kit (Qiagen Inc., USA) in a 20 µl reaction, respectively. An RT-minus negative control reaction with all the components for the RT reaction (except the Reverse Transcriptase enzyme) was carried out for each sample to control genomic DNA contamination. The RT-qPCR runs were performed in triplicates for each sample using the StepOnePlus™ (Applied Biosystems®, Life Technologies, USA). To evaluate the transcriptional level, comparative $2^{-\Delta\Delta Ct}$ method was applied according Livak and Schmittgen (2001) using Elongation factor alpha (Valenzuela-Muñoz and Gallardo-Escárate, 2017) and Ssa-mir-455-5p (Johansen and Andreassen, 2014) as reference transcripts for mRNAs and miRNAs, respectively. Reactions were conducted with a volume of 10 µL using the Maxima® SYBR Green/ROX qPCR Master Mix (Thermo Scientific, USA) and miScript SYBR Green PCR Kit (Qiagen, USA) for mRNA and miRNAs, respectively. The amplification cycle was as follows: 95 °C for 10 min, 40 cycles at 95°C for 15s, and 60°C for 1 min, followed by a disassociation curve under the same conditions. The efficiency of the primers was calculated and reported according MIQE guidelines (Bustin et al., 2009). Finally, all data was checked for normality using the Shapiro-Wilk test. Data not meeting this criteria were normalized through BoxCox transformation (Westfall and Henning, 2013). Statistical differences in expression data were evaluated using a one-way ANOVA (analysis of variance), followed by Tukey's multiple comparison tests using the JMP v9 software (SAS Institute Inc., USA). Statistically significant differences were accepted with a $p < 0.05$.

3. Results

3.1 Identification of miRNA in Atlantic salmon

213 After adapter trimming, 12,986,381 and 18,068,288 reads were obtained respectively from
214 Atlantic salmon skin and head kidney. In total, 62,182 small RNA clean reads were
215 identified from skin and head kidney (Table 1), which were annotated using sequences
216 available in miRBase 21 (http://www.mirbase.org) for *Salmo salar, Danio rerio, Cyprinus*
217 *carpio, Ictalurus punctatus* and *Fugu rubripes*, yielding a total of 1,718 annotated
218 miRNAs. The average length for all annotated miRNAs was 21-23 nucleotide (Fig. 1A).
219 Several isoforms or isomiRs of mature 5´and mature 3´ precursors were found, the most
220 abundant variants being mapped to mature 5' and mature 3' sequences (Fig. 1B). miRNAs
221 were classified into several families, the most abundant in salmon infested with sea lice
222 being mir-10, mir-181 and mir-21, mir-30 and let7 (Fig. 1C). The analysis of skin and head
223 kidney tissue revealed significant differences between them in the number of annotated
224 miRNAs, with a total of 529 and 1,404 transcripts, respectively (Table 1). Moreover,
225 comparative sequence analysis identified 486 miRNAs shared between the two types of
226 tissue, while 43 and 918 were identified as only in skin and head kidney, respectively (Fig.
227 1D). Among the miRNAs only in skin tissue, the most abundant families were mir-203,
228 mir-499, mir-148, while the most abundant in head kidney were mir-731, mir-202, and mir-
229 144 (Table S1). Some miRNA families were like mir-196, mir-133, mir-99 and mir206
230 were related only to skin tissue, while mir-1388, mir-223a and mir-551 families were only
231 associated with head kidney (Table S1).
232
233 *3.2 Modulation of miRNA profiles in Atlantic salmon tissue during sea louse infestation*
234 Using the 1,718 miRNAs identified in Atlantic salmon, RNA-seq analysis compared
235 changes in miRNA expression in skin and head kidney during the sea louse infestation.
236 Heat-map representation showed different expression profiles of miRNAs over the course

237 of infestation (Fig. 2). Clustering analysis using Euclidian distances showed families of
238 miRNAs that were differentially expressed between tissues and among post-infection days
239 (Table S2). Seven clusters were identified in skin tissue from the infected area (Fig. 2A). A
240 large number of miRNAs of the mir-10, mir-21, mir-181 and mir-462 families were
241 observed in these clusters (Fig. 2B). The expression patterns in the clusters differed during
242 *C. rogercresseyi* infestation, for instance, clusters 1 and 4 were highly regulated before
243 infestation and 14 dpi; cluster 2, 3 and 7 were highly regulated before infestation.
244 Moreover, cluster 5 was upregulated at 14 dpi, showing an enrichment of mir-143, mir-199
245 and mir-2184 families (Fig. 2B). 2Nine clusters were detected in head kidney, two of them,
246 cluster 1 and 8, with high expression values at 14 dpi, while cluster 3 and 5 were also
247 upregulated at 14 dpi (Fig. 2C). Cluster 2-7 showed low expression at 7 dpi. Furthermore,
248 the most enriched miRNA families were mir-26, mir-21, mir-181, mir-10 and mir-462 (Fig
249 2C, 2D).

250 Statistical analyses were conducted with skin and head kidney of infected Atlantic
251 salmon to detect differentially expressed miRNAs (Fig 3). Thirteen miRNAs differently
252 regulated at 14pdi in skin and seventy-one miRNA were differently regulated 7 dpi in head
253 kidney (Fig. 3, Table S3). Notably, miRNome of Atlantic salmon skin 7 and 9 miRNAs
254 exclusively expressed at 7 dpi and 14 dpi (Fig 3A), while 69 and 3 miRNAs from head
255 kidney tissue were highly regulated during the sea louse infestation. Two miRNAs were
256 regulated at 7 and 14 dpi in head kidney (Fig 3B). Analysis of the correlation expression of
257 miRNAs revealed a high degree of correlation among specific miRNAs (Fig. 4). Pairwise
258 comparison revealed a conspicuous clusters with correlation values >0.8 (Table S4). Skin
259 transcriptome showed low a number of significant correlations among the tested miRNAs,
260 where the most abundant transcripts, mir-462, mir-21 and mir-181, had positive

261 correlations (Fig. 4A). In contrast, a large number of miRNAs were significantly expressed
262 in head kidney (Fig. 4B). For instance, mir-142 and mir-181 families showed positive
263 correlations with let-7, mir-10a, mir-126a, mir-130a, mir-143, mir-30b and mir-30c
264 families (Fig. 4B). Correlation analysis was also conducted to evaluate co-expression
265 patterns among miRNAs and mRNAs highly expressed during the *C. rogercresseyi*
266 infection. Notably, genes related to iron regulation and immune response correlated
267 positively with the miRNAs analyzed previously (Fig. 1S).
268
269 *3.3 Atlantic salmon miRNome and immune response against sea lice*
270 Five immune-related genes (*TLR12, MMP13, COX2, IFNg, CCR3*), three iron transport
271 genes (*haptoglobin, ferritin H, IRP2*) and three heme biosynthesis-related genes (*ALAs,*
272 *HO, BLVr*) were evaluated as putative target genes to determine the role of miRNAs in
273 Atlantic salmon in response to *C. rogercresseyi* infestation. These genes have evidenced
274 high modulation in Atlantic salmon in response to sea louse infestation. Using target gene
275 prediction analyses to determine the binding sites, we found low levels of free energy in
276 mir-140-4, mir-181a-5-2, mir-10b-19, mir-126-03, mir-21-2 and 3'UTRs of the immune
277 genes *TLR12, MMP13, COX2, IFNg* and *CCR3*, respectively (Fig. 5A). RT-qPCR analysis
278 was applied using the fold-change values of immune-related genes from skin and head
279 kidney to evaluate the miRNA expression with their putative target genes. Overall, there is
280 an inverse relationship between miRNA expression and target genes during sea louse
281 infestation (Fig. 5C-D), suggesting putative modulation of these immune-related genes
282 mediated through miRNAs. Furthermore, a key role of iron regulation has been reported in
283 Atlantic salmon in response to sea louse infestation and particularly related to nutritional
284 immunity (Valenzuela-Muñoz and Gallardo-Escárate, 2017). Low levels of duplex-free

energy were estimated from bioinformatic target gene prediction for mir-1338, let-7c-1, mir-124a-1, mir-181a-2-5, mir-10b-4-3 and let7d-1 binding to *haptoglobin, ferritin H, IRP2, ALAs, HO* and *BLVr* genes (Fig. 6A). Expression analysis of these miRNAs and their putative iron regulation-related genes showed inverse transcription patterns in tissue infected with sea lice (Fig. 6C-D). However, the transcription analysis evidenced tissue-specific patterns in the miRNA/mRNA expression paterns, suggesting that the molecular mechanism of miRNAs is influenced at the same time by the transcriptional activity expressed during the sea lice infestation. Finally, RT-qPCR corroborated the *in silico* results of this study. No similarities were observed in expression patterns between the *in silico* and RT-qPCR analyses in skin tissue (Fig 7). However, RT-qPCR analysis showed distinct expression patterns between miRNA and target genes in Atlantic salmon skin, as was expected (Fig. 7). A high level of correspondence was observed between TPM and the relative expression values of head kidney miRNA, and an opposite expression pattern was observed with its target gene (Fig 7).

4. Discussion

The increasing use in recent years of new generation sequencing in animal biology has improved our understanding of the molecular mechanisms that modulate transcriptomes related to key biological processes. For instance, non-coding RNA and miRNAs have emerged as pivotal regulators of the immune response, playing important roles during host/pathogen interactions (Bi et al., 2009; Hussain and Asgari, 2014; Lindsay, 2008). To the best of our knowledge, this study is the first to apply small RNA sequencing to identify miRNA expression profiles in Atlantic salmon during sea louse infestation and to evaluate putative miRNA target genes related to the immune response against *C. rogercresseyi.* A

309 total of 62,182 small RNAs were identified from small RNA libraries constructed from skin
310 and head kidney tissue of infected fish. Here, using miRBase we annotated 1,718
311 transcripts with a high percentage of small RNAs annotated to miRNAs previously reported
312 for *Salmo salar*. As in similar studies of other fish species, the most abundant transcripts
313 belonging to mir-181, mir-21 and let-7 families were identified (Bekaert et al., 2013;
314 Farlora et al., 2015; Salem et al., 2010; Sha et al., 2014).

315 MiRNAs are highly conserved among vertebrates and invertebrates. They have the
316 capacity to regulate more than one target gene, making it possible to modulate the
317 expression of several genes in different tissues (Lagos-Quintana et al., 2002; Wang et al.,
318 2016). For instance, comparison of expression levels in samples from different Atlantic
319 salmon tissue evidenced tissue-specific expression differences in three conserved and one
320 novel miRNA. Here, Ssa-miR 736 was only detected in heart tissue, while two other
321 clustered miRNAs (ssa-miR 212 and132) seems to have higher expression levels in brain
322 tissue. Differential expression analysis using DESeq suggests that Ssa-miR 8163 is
323 enriched in liver tissue and putatively regulates the transferrin gene (Andreassen et al.,
324 2013). In the present study, a higher number of miRNAs were annotated in head kidney
325 than in skin tissue. Some miRNAs were only identified in tissue infected with sea lice. For
326 example, mir-196, which has previously only been reported in the head kidney tissue of
327 rainbow trout (Salem et al., 2010), was only expressed in our study in Atlantic salmon skin.
328 We found miRNAs that are exclusive to head kidney, such as mir-1388 and mir-155. These
329 transcripts have been described as critical in erythropoiesis in Antarctic fish, modulating
330 genes involved in the TGF-b pathway (Xu et al., 2015). In turn, the expression of mir-1388
331 and mir-155 in Atlantic salmon head kidney indicate conserved functions related to blood
332 cell lineages.

333 Changes in miRNA expression levels were detected in different tissue and at
334 different sampling times during infestation with sea lice. For example, *Cynoglossus*
335 *semilaevis* infected with *Vibrio anguillarum* showed variation in the expression levels of
336 mir-142-5p, mir-223 and mir-181a in spleen, head kidney, intestine and liver tissues,
337 suggesting that bacterial infestation modulate miRNA expression differently, depending on
338 the target tissue of infection (Gong et al., 2015). Recent studies with tilapia have shown
339 differences in expression profiles of miRNAs after 72 h of *Streptococcus agalactiae*
340 infection, with downregulation of mir-214, mir-155 and mir-29 at early infection stages
341 (Wang et al., 2016). Similarly, *Paralichthys olivaceus* infected with VHSV revealed higher
342 expression levels of mir-146a and mir-155 at 48 h post-infection (Najib et al., 2016). Our
343 results show differences in miRNA expression patterns between skin and head kidney of
344 Atlantic salmon after *C. rogercresseyi* infestation. A significant number of highly regulated
345 miRNAs was detected in head kidney at 7 dpi, contrasting with the skin tissue miRNA
346 expression profile. Keeping in mind that the function of miRNAs is to interfere with the
347 transcription activity of their target genes (Bartel, 2004; Bartel, 2009) and the large number
348 of highly regulated coding transcripts in skin and head kidney at 7 and 14 dpi, respectively
349 (Valenzuela-Muñoz et al., 2016), we hypothesize that the high number of miRNA regulated
350 in head kidney at 7 dpi are turning-off the coding-transcripts in Atlantic salmon at early
351 stages of sea louse infestation. Our results indicate that the skin transcriptome, as the target
352 tissue for this ectoparasite, requires downregulation by miRNAs to trigger the immune
353 response against sea lice.

354 RNA-seq analysis of Atlantic salmon infested with *C. rogercresseyi* evidenced
355 exclusive miRNA clusters during infestation. Notably, all the clusters have been reported as
356 conservative miRNAs across vertebrate species. One is mir-181, which regulates

hematopoiesis and T-lymphocyte maturation (Xiao and Rajewsky, 2009). Mir-181 and mir-21 in humans activates inflammatory cytokines like STAT-3 and IL6 in the presence of cancer (Iliopoulos et al., 2010). Mir-10 is another highly abundant miRNA that regulates *Hox* genes (Woltering and Durston, 2008). Mir-10 has been described as highly regulated in coelomocytes of sea cumbers with skin ulcers (Sun et al., 2016). Mir-462 was also present in all the clusters we identified for Atlantic salmon skin and head kidney. Mir-462 has been observed highly modulated in fish during viral (Bela-ong et al., 2013) and bacterial infections (Gong et al., 2015), which suggests that immune regulation in Atlantic salmon is modulated through conserved miRNAs independent of the parasite. Indeed, miRNAs can regulate lymphocyte differentiation, monocyte proliferation, inflammatory response, and toll-like receptor signalling, among other immune processes (Baltimore et al., 2008; Lindsay, 2008; Lu and Liston, 2009; O'Neill et al., 2011). The response of Atlantic salmon to *C. rogercresseyi* infestation has been associated with immune aspects like Th1-type response, toll like receptor activation (TLR22a) and nutritional immunity related to iron availability (Boltaña et al., 2016; Valenzuela-Muñoz et al., 2016; Valenzuela-Muñoz and Gallardo-Escárate, 2017). MiRNAs have the capacity to reduce the RNA stability by imperfect binding to the 3'UTR region of target genes (Lindsay, 2008). Gene target prediction was conducted to associate this feature with the immune response in Atlantic salmon and the analyzed miRNAs. The high level of expression of mir-140 in head kidney at 7 dpi was correlated with downregulation of the *TLR22* gene. This cell receptor is involved in fish response to sea louse infestation (Panda et al., 2014; Valenzuela-Muñoz et al., 2016). Atlantic salmon infected with *Lepeophtheirus salmonis* have been described as having a Th2 type immune response. However, this type of response has been not observed in Atlantic salmon infected with *C. rogercresseyi* (Valenzuela-Muñoz et al., 2016).

Furthermore, in our analysis, we identified significantly upregulated miRNA that targets the CCR3 gene involved in Th2 response. With respect to nutritional immunity, heme degradation increases in Atlantic salmon infected with *C. rogercresseyi* (Valenzuela-Muñoz and Gallardo-Escárate, 2017). In the present study, we observed high levels of mir-181a-2-5 expression, which seems to modulate the ALAs gene involved in heme biosynthesis, suggesting that mir-181a-2-5 allows free iron to increase as a consequence of heme degradation.

5. Conclusion

This is the first study to relate miRNA profiles of Atlantic salmon to an ectoparasite species like the sea louse *C. rogercresseyi*. We report differences in miRNA expression signatures during infestation, with a high number of miRNAs regulated in head kidney in early infestation. Furthermore, gene target prediction analysis revealed strong relationships between miRNA expression and candidate genes involved in immune system response and iron regulation. However, further functional analyses are required to validate their molecular role during sea louse infection. The present work offers a valuable resource that, combined with functional studies, will foster the development of novel therapeutic tools in fish aquaculture.

6. Acknowledgments

This study was funded by CONICYT-Chile through the grants FONDAP (1510027), FONDECYT (1150077) and PCHA/Doctorado Nacional/2016-21161036.

7. References

405
406 Andreassen, R., Worren, M.M., Høyheim, B., 2013. Discovery and characterization of
407 miRNA genes in Atlantic salmon (*Salmo salar*) by use of a deep sequencing approach.
408 BMC genomics 14, 482.
409 Baltimore, D., Boldin, M.P., O'Connell, R.M., Rao, D.S., Taganov, K.D., 2008.
410 MicroRNAs: new regulators of immune cell development and function. Nature
411 immunology 9, 839-845.
412 Barozai, M.Y.K., 2012. Identification and characterization of the microRNAs and their
413 targets in *Salmo salar*. Gene 499, 163-168.
414 Bartel, D.P., 2004. MicroRNAs: Genomics, Biogenesis, Mechanism, and Function. Cell
415 116, 281-297.
416 Bartel, D.P., 2009. MicroRNAs: target recognition and regulatory functions. cell 136, 215-
417 233.
418 Bekaert, M., Lowe, N.R., Bishop, S.C., Bron, J.E., Taggart, J.B., Houston, R.D., 2013.
419 Sequencing and characterisation of an extensive Atlantic salmon (*Salmo salar* L.)
420 microRNA repertoire. PLoS One 8, e70136.
421 Bela-ong, D.B., Schyth, B.D., Lorenzen, N., 2013. Evaluation of the potential anti-viral
422 activity of microRNAs in rainbow trout (*Oncorhynchus mykiss*). Fish & Shellfish
423 Immunology 34, 1639.
424 Bi, Y., Liu, G., Yang, R., 2009. MicroRNAs: novel regulators during the immune response.
425 Journal of cellular physiology 218, 467-472.
426 Boltaña, S., Sanchez, M., Valenzuela, V., Gallardo-Escárate, C., 2016. Density-dependent
427 effects of *Caligus rogercresseyi* infestation on the immune responses of *Salmo salar*.
428 Fish & Shellfish Immunology 59, 365-374.
429 Bushati, N., Cohen, S.M., 2007. microRNA functions. Annu. Rev. Cell Dev. Biol. 23, 175-
430 205.
431 Bustin, S.A., Benes, V., Garson, J.A., Hellemans, J., Huggett, J., Kubista, M., Mueller, R.,
432 Nolan, T., Pfaffl, M.W., Shipley, G.L., Vandesompele, J., Wittwer, C.T., 2009. The
433 MIQE Guidelines: Minimum Information for Publication of Quantitative Real-Time
434 PCR Experiments. Clin Chem 55, 611-622.
435 Chen, C.-Z., Li, L., Lodish, H.F., Bartel, D.P., 2004. MicroRNAs modulate hematopoietic
436 lineage differentiation. science 303, 83-86.
437 Davidson-Moncada, J., Papavasiliou, F.N., Tam, W., 2010. MicroRNAs of the immune
438 system. Annals of the New York Academy of Sciences 1183, 183-194.
439 Farlora, R., Valenzuela-Miranda, D., Alarcon-Matus, P., Gallardo-Escarate, C., 2015.
440 Identification of microRNAs associated with sexual maturity in Rainbow Trout brain
441 and testis through small RNA deep sequencing. Mol. Reprod. Dev. 82, 651-662.
442 Fast, M.D., 2014. Fish immune responses to parasitic copepod (namely sea lice) infection.
443 Dev. Comp. Immunol. 43, 300-312.
444 Gong, G., Sha, Z., Chen, S., Li, C., Yan, H., Chen, Y., Wang, T., 2015. Expression
445 profiling analysis of the microRNA response of *Cynoglossus semilaevis* to *Vibrio*
446 *anguillarum* and other stimuli. Marine Biotechnology 17, 338-352.
447 González, L., Carvajal, J., 2003. Life cycle of *Caligus rogercresseyi*, (Copepoda:
448 Caligidae) parasite of Chilean reared salmonids. Aquaculture 220, 101-117.
449 Hussain, M., Asgari, S., 2014. MicroRNAs as mediators of insect host–pathogen
450 interactions and immunity. Journal of insect physiology 70, 151-158.

Iliopoulos, D., Jaeger, S.A., Hirsch, H.A., Bulyk, M.L., Struhl, K., 2010. STAT3 Activation of miR-21 and miR-181b-1 via PTEN and CYLD Are Part of the Epigenetic Switch Linking Inflammation to Cancer. Molecular Cell 39, 493-506.

Johansen, L., Andreassen, R., 2014. Validation of miRNA genes suitable as reference genes in qPCR analyses of miRNA gene expression in Atlantic salmon (Salmo salar). BMC Research Notes 7, 1-9.

John, B., Enright, A.J., Aravin, A., Tuschl, T., Sander, C., Marks, D.S., 2004. Human MicroRNA targets. Plos Biol 2, 1862-1879.

Judice, C.C., Bourgard, C., Kayano, A.C., Albrecht, L., Costa, F.T., 2016. MicroRNAs in the host-apicomplexan parasites interactions: a review of immunopathological aspects. Frontiers in cellular and infection microbiology 6, doi: 10.3389/fcimb.2016.00005.

Kertesz, M., Iovino, N., Unnerstall, U., Gaul, U., Segal, E., 2007. The role of site accessibility in microRNA target recognition. Nat Genet 39, 1278-1284.

Kozomara, A., Griffiths-Jones, S., 2011. miRBase: integrating microRNA annotation and deep-sequencing data. Nucleic Acids Res 39, D152-D157.

Kozomara, A., Griffiths-Jones, S., 2014. miRBase: annotating high confidence microRNAs using deep sequencing data. Nucleic Acids Res 42, D68-D73.

Kure, E.H., Sæbø, M., Stangeland, A.M., Hamfjord, J., Hytterød, S., Heggenes, J., Lydersen, E., 2013. Molecular responses to toxicological stressors: Profiling microRNAs in wild Atlantic salmon (*Salmo salar*) exposed to acidic aluminum-rich water. Aquatic Toxicology 138–139, 98-104.

Lagos-Quintana, M., Rauhut, R., Yalcin, A., Meyer, J., Lendeckel, W., Tuschl, T., 2002. Identification of Tissue-Specific MicroRNAs from Mouse. Current Biology 12, 735-739.

Lindsay, M.A., 2008. microRNAs and the immune response. Trends in immunology 29, 343-351.

Livak, K.J., Schmittgen, T.D., 2001. Analysis of relative gene expression data using real-time quantitative PCR and the 2(T)(-Delta Delta C) method. Methods 25, 402-408.

Lu, L.F., Liston, A., 2009. MicroRNA in the immune system, microRNA as an immune system. Immunology 127, 291-298.

Najib, A., Kim, M.S., Choi, S.H., Kang, Y.J., Kim, K.H., 2016. Changes in microRNAs expression profile of olive flounder (*Paralichthys olivaceus*) in response to viral hemorrhagic septicemia virus (VHSV) infection. Fish & Shellfish Immunology 51, 384-391.

O'Connell, R.M., Rao, D.S., Baltimore, D., 2012. microRNA regulation of inflammatory responses. Annual review of immunology 30, 295-312.

O'Neill, L.A., Sheedy, F.J., McCoy, C.E., 2011. MicroRNAs: the fine-tuners of Toll-like receptor signalling. Nature Reviews Immunology 11, 163-175.

Ou, J., Meng, Q., Li, Y., Xiu, Y., Du, J., Gu, W., Wu, T., Li, W., Ding, Z., Wang, W., 2012. Identification and comparative analysis of the *Eriocheir sinensis* microRNA transcriptome response to *Spiroplasma eriocheiris* infection using a deep sequencing approach. Fish & shellfish immunology 32, 345-352.

Panda, R.P., Chakrapani, V., Patra, S.K., Saha, J.N., Jayasankar, P., Kar, B., Sahoo, P.K., Barman, H.K., 2014. First evidence of comparative responses of Toll-like receptor 22 (TLR22) to relatively resistant and susceptible Indian farmed carps to *Argulus siamensis* infection. Developmental & Comparative Immunology 47, 25-35.

Rennie, W., Liu, C.C., Carmack, C.S., Wolenc, A., Kanoria, S., Lu, J., Long, D., Ding, Y., 2014. STarMir: a web server for prediction of microRNA binding sites. Nucleic Acids Res 42, W114-W118.

Salem, M., Xiao, C., Womack, J., Rexroad, C.E., Yao, J., 2010. A microRNA repertoire for functional genome research in Rainbow Trout (*Oncorhynchus mykiss*). Marine Biotechnology 12, 410-429.

Sha, Z., Gong, G., Wang, S., Lu, Y., Wang, L., Wang, Q., Chen, S., 2014. Identification and characterization of *Cynoglossus semilaevis* microRNA response to *Vibrio anguillarum* infection through high-throughput sequencing. Developmental & Comparative Immunology 44, 59-69.

Sonkoly, E., Ståhle, M., Pivarcsi, A., 2008. MicroRNAs and immunity: novel players in the regulation of normal immune function and inflammation, Seminars in cancer biology. Elsevier, pp. 131-140.

Sun, H., Zhou, Z., Dong, Y., Yang, A., Jiang, J., Chen, Z., Guan, X., Wang, B., Gao, S., Jiang, B., 2016. Expression analysis of microRNAs related to the skin ulceration syndrome of sea cucumber *Apostichopus japonicus*. Fish & shellfish immunology 49, 205-212.

Taganov, K.D., Boldin, M.P., Chang, K.-J., Baltimore, D., 2006. NF-κB-dependent induction of microRNA miR-146, an inhibitor targeted to signaling proteins of innate immune responses. Proceedings of the National Academy of Sciences 103, 12481-12486.

Valenzuela-Muñoz, V., Boltaña, S., Gallardo-Escárate, C., 2016. Comparative immunity of *Salmo salar* and *Oncorhynchus kisutch* during infestation with the sea louse *Caligus rogercresseyi*: An enrichment transcriptome analysis. Fish & Shellfish Immunology 59, 276-287.

Valenzuela-Muñoz, V., Gallardo-Escárate, C., 2017. Iron metabolism modulation in *Atlantic salmon* infested with the sea lice *Lepeophtheirus salmonis* and *Caligus rogercresseyi*: A matter of nutritional immunity? Fish & Shellfish Immunology 60, 97-102.

Wagner, G.P., Kin, K., Lynch, V.J., 2012. Measurement of mRNA abundance using RNA-seq data: RPKM measure is inconsistent among samples. Theor Biosci 131, 281-285.

Wang, B., Gan, Z., Cai, S., Wang, Z., Yu, D., Lin, Z., Lu, Y., Wu, Z., Jian, J., 2016. Comprehensive identification and profiling of Nile tilapia (*Oreochromis niloticus*) microRNAs response to *Streptococcus agalactiae* infection through high-throughput sequencing. Fish & shellfish immunology 54, 93-106.

Westfall, P., Henning, K.S., 2013. Understanding advanced statistical methods. CRC Press.

Woltering, J.M., Durston, A.J., 2008. MiR-10 Represses HoxB1a and HoxB3a in Zebrafish. PLOS ONE 3, e1396.

Xiao, C., Rajewsky, K., 2009. MicroRNA control in the immune system: basic principles. Cell 136, 26-36.

Xu, Q., Cai, C., Hu, X., Liu, Y., Guo, Y., Hu, P., Chen, Z., Peng, S., Zhang, D., Jiang, S., 2015. Evolutionary suppression of erythropoiesis via the modulation of TGF-β signalling in an Antarctic icefish. Molecular ecology 24, 4664-4678.

Table 1. Summary of small RNA sequencing in Atlantic salmon infected with *Caligus rogercresseyi.*

Tissue	**Skin**	**Head kidney**	**Total**
Number of reads	21,213,927	29,865,990	51,079,917
Average length (nt)	41	41	41
Number of reads after trimmed	12,986,381	18,068,288	31,054,669
Average length after trimming (nt)	21	21	21
Number of small RNA annotated	529	1,404	1,718

Figure List

Figure 1. Identification and annotation of Atlantic salmon miRNAs using sRNA-sequencing. A) Size distribution of Atlantic salmon miRNAs after trimming and mapping against miRBase 21, C) Number of isomiRs 5´- 3´and precursor variants identified in the Atlantic salmon transcriptome, D) Venn diagram of the number of miRNA annotated for Atlantic salmon skin and head kidney.

Figure 2. Transcriptome profiles of miRNAs for skin and head kidney of Atlantic salmon infested with *C. rogercresseyi.* A: Clustering analysis for skin during sea lice infestation. B: Graphical representation for more abundant miRNA founding in skin by cluster. C: Clustering analysis for head kidney during sea lice infestation. D: Graphical representation for more abundant miRNA founding in head kidney by cluster.

Figure 3. Veen diagrams of differentially expressed miRNAs among infestation process in Atlantic salmon. A) Comparison in Atlantic salmon skin T0 vs. T7, and T0 vs. T14, respectively, and B) Comparison in Atlantic salmon head kidney T0 vs. T7, and T0 vs. T14. Each box shows the miRNAs exclusives and shared for each pairwise comparison. Red and green bars represent the fold-changes values, up and downregulated, respectively (p-value 0.05 and fold change $|1|$). * The eight top regulated miRNA for T0vs T7 in head kidney samples were include in the figure.

Figure 4. Correlation plot matrix between miRNA differently expressed in skin (A) and head kidney (B) of Atlantic salmon infested with *C. rogercresseyi*. Color scale represents the correlation values.

Figure 5. miRNA target prediction for immune-related genes in Atlantic salmon infested with *C. rogercresseyi*. A) Schematic representation of immune-related mRNAs and predicted pairing of miRNAs on 3´ UTRs, and B) Atlantic salmon skin fold changes by *in silico* analysis for miRNA and fold change profiling by RT-qPCR of their putative predict target genes. C) Atlantic salmon head kidney fold changes by *in silico* analysis for miRNA and fold change profiling by RT-qPCR of their putative predict target genes.. (* indicated significant differences between sample points $p<0.05$)

Figure 6. miRNA target prediction for iron transport genes and heme biosynthesis/degradation pathways in Atlantic salmon infested with *C. rogercresseyi*. A) Schematic representation of iron modulation-related mRNAs of and predicted pairing of miRNAs on 3´ UTRs, B) *In silico* fold changes values of Atlantic salmon skin miRNA and fold change profiling by RT-qPCR of their putative predict target genes. C) *In silico* fold changes values of Atlantic salmon head kidney miRNA and fold change profiling by RT-qPCR of their putative predict target genes. (* indicated significant differences between sample points $p<0.05$)

Figure 7. RT-qPCR validation of miRNAs and putative target genes identified in Atlantic salmon transcriptome infected with *C. rogercresseyi*.

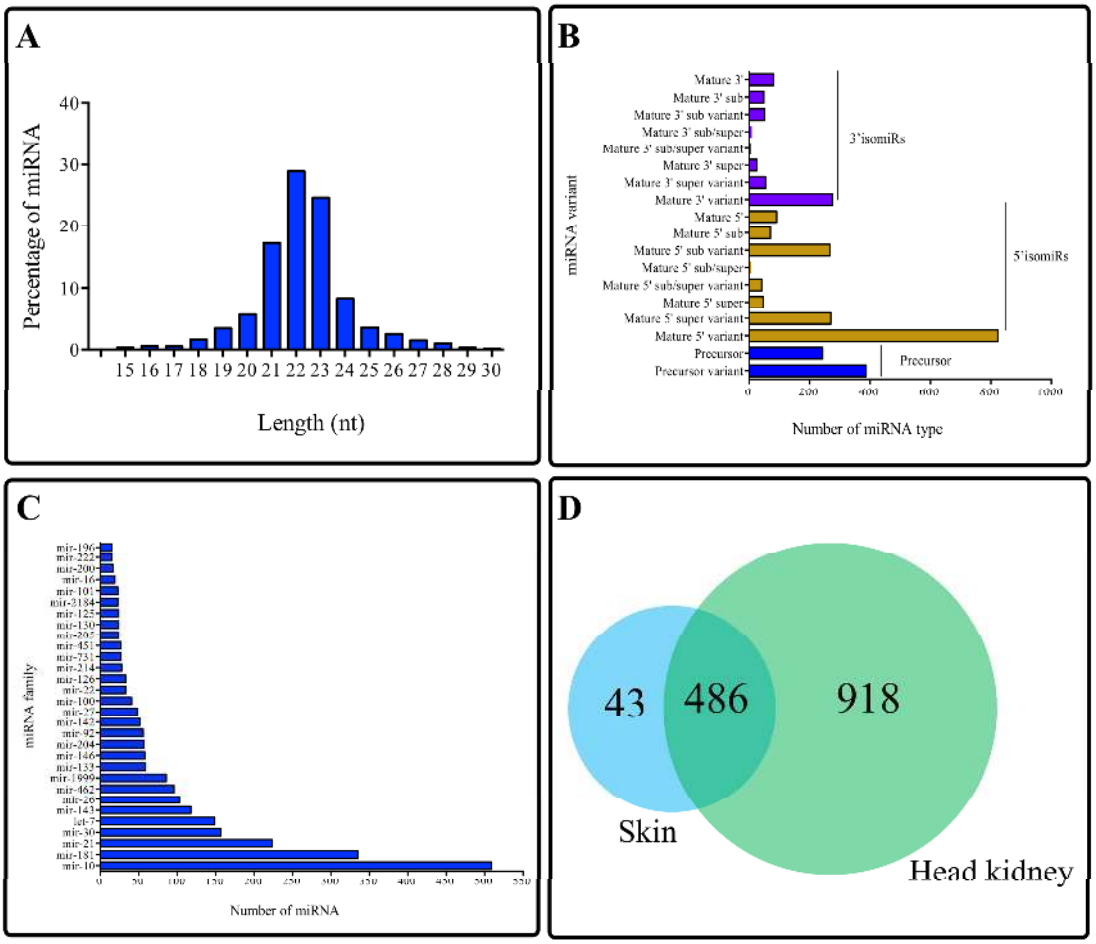

Figure 1

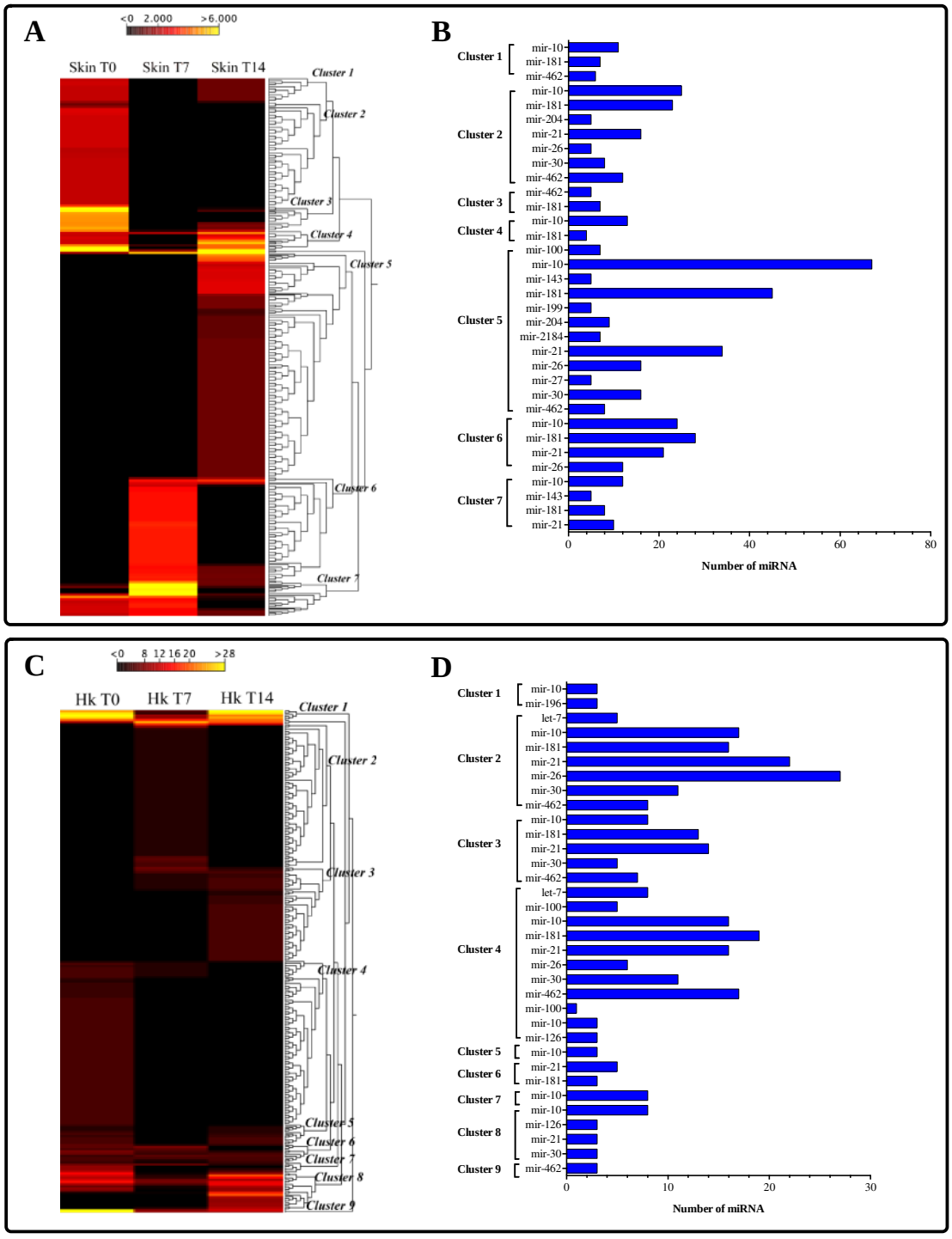
A
<0 2.000 >6.000
Skin T0
Skin T7
Skin T14
Cluster 1
Cluster 2
Cluster 3
Cluster 4
Cluster 5
Cluster 6
Cluster 7
B
Cluster 1
mir-10
mir-181
mir-462
Cluster 2
mir-10
mir-181
mir-204
mir-21
mir-26
mir-30
mir-462
Cluster 3
mir-462
mir-181
Cluster 4
mir-10
mir-181
Cluster 5
mir-100
mir-10
mir-143
mir-181
mir-199
mir-204
mir-2184
mir-21
mir-26
mir-27
mir-30
mir-462
Cluster 6
mir-10
mir-181
mir-21
mir-26
Cluster 7
mir-10
mir-143
mir-181
mir-21
0
20
40
60
80
Number of miRNA
C
<0 8 12 16 20 >28
Hk T0
Hk T7
Hk T14
Cluster 1
Cluster 2
Cluster 3
Cluster 4
Cluster 5
Cluster 6
Cluster 7
Cluster 8
Cluster 9
D
Cluster 1
mir-10
mir-196
Cluster 2
let-7
mir-10
mir-181
mir-21
mir-26
mir-30
mir-462
Cluster 3
mir-10
mir-181
mir-21
mir-30
mir-462
Cluster 4
let-7
mir-100
mir-10
mir-181
mir-21
mir-26
mir-30
mir-462
mir-100
mir-10
mir-126
Cluster 5
mir-10
Cluster 6
mir-21
mir-181
Cluster 7
mir-10
mir-10
Cluster 8
mir-126
mir-21
mir-30
Cluster 9
mir-462
0
10
20
30
Number of miRNA

Figure 2

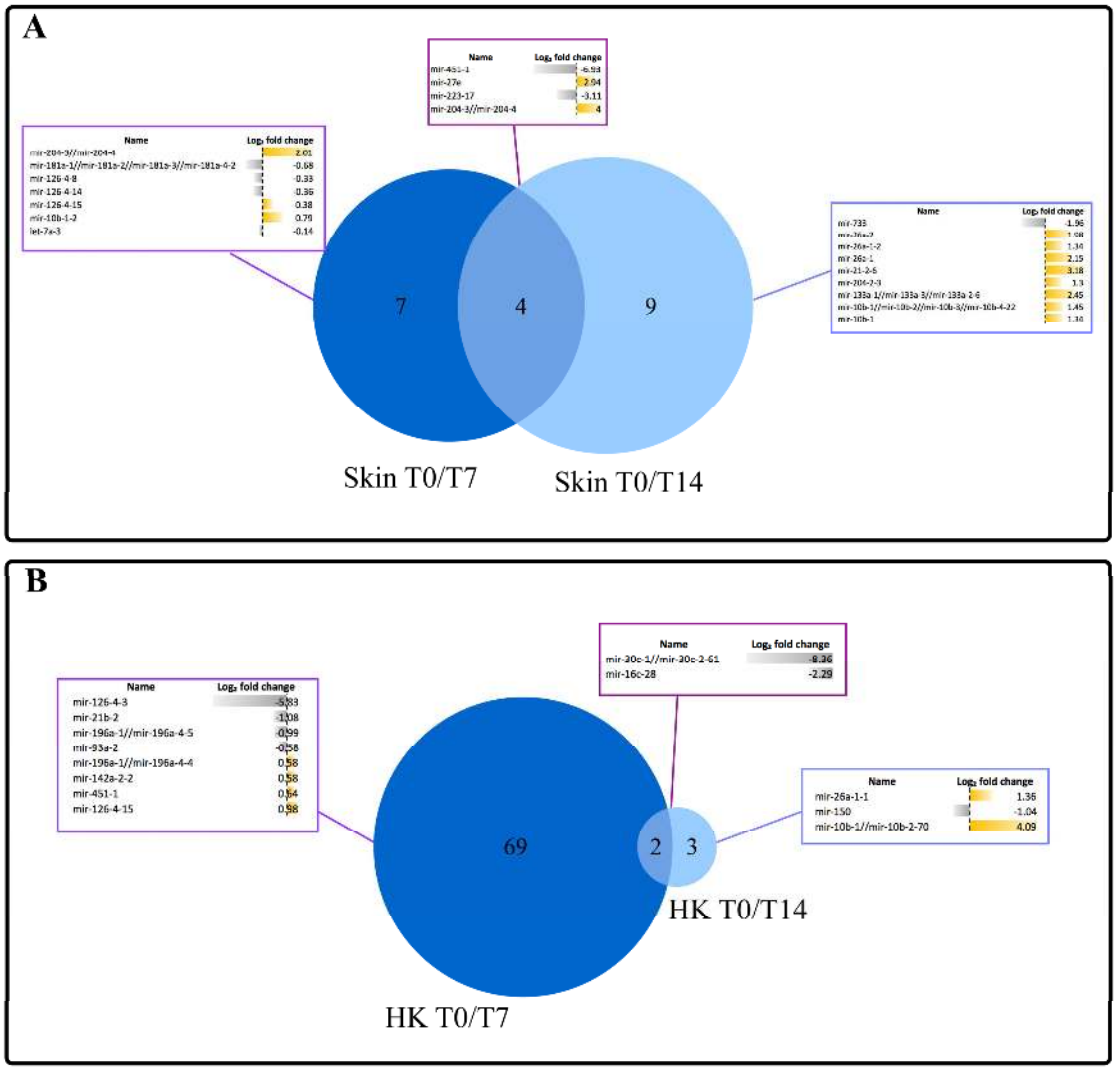

Figure 3

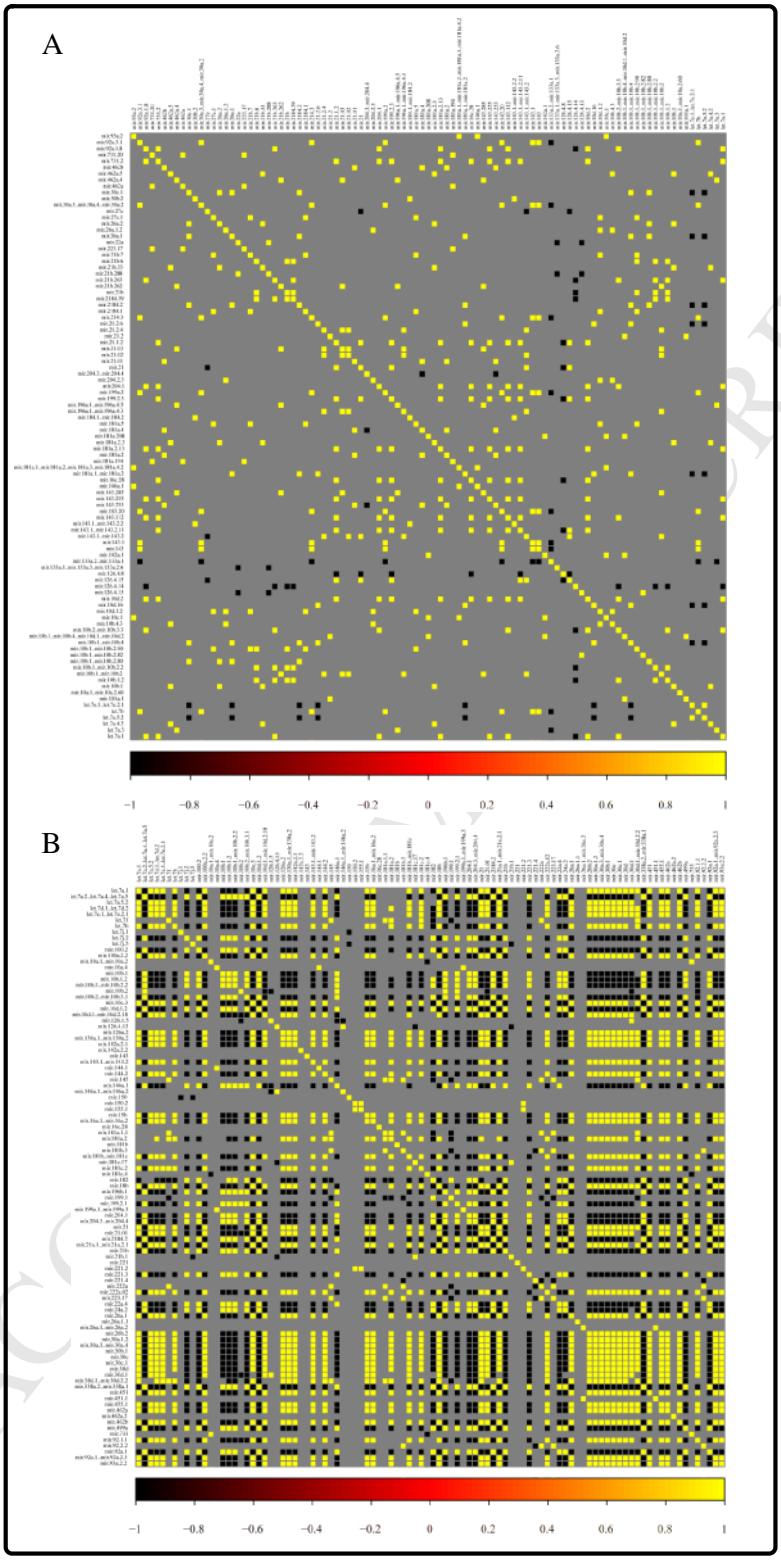

Figure 4

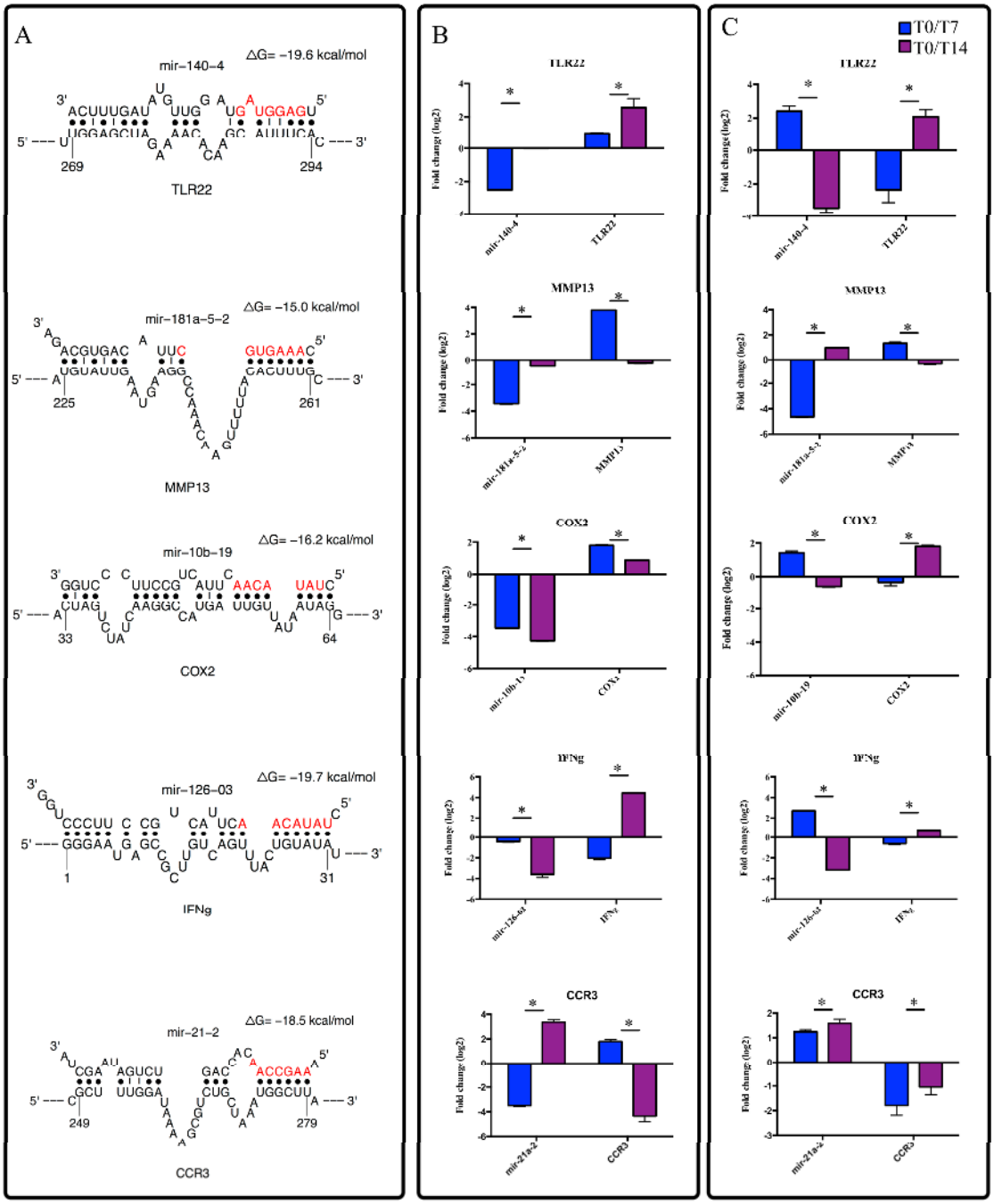
A
mir–140–4
ΔG= –19.6 kcal/mol
TLR22
mir–181a–5–2
ΔG= –15.0 kcal/mol
MMP13
mir–10b–19
ΔG= –16.2 kcal/mol
COX2
mir–126–03
ΔG= –19.7 kcal/mol
IFNg
mir–21–2
ΔG= –18.5 kcal/mol
CCR3
B
C
T0/T7
T0/T14
TLR22
MMP13
COX2
IFNg
CCR3
Fold change (log2)

Figure 5

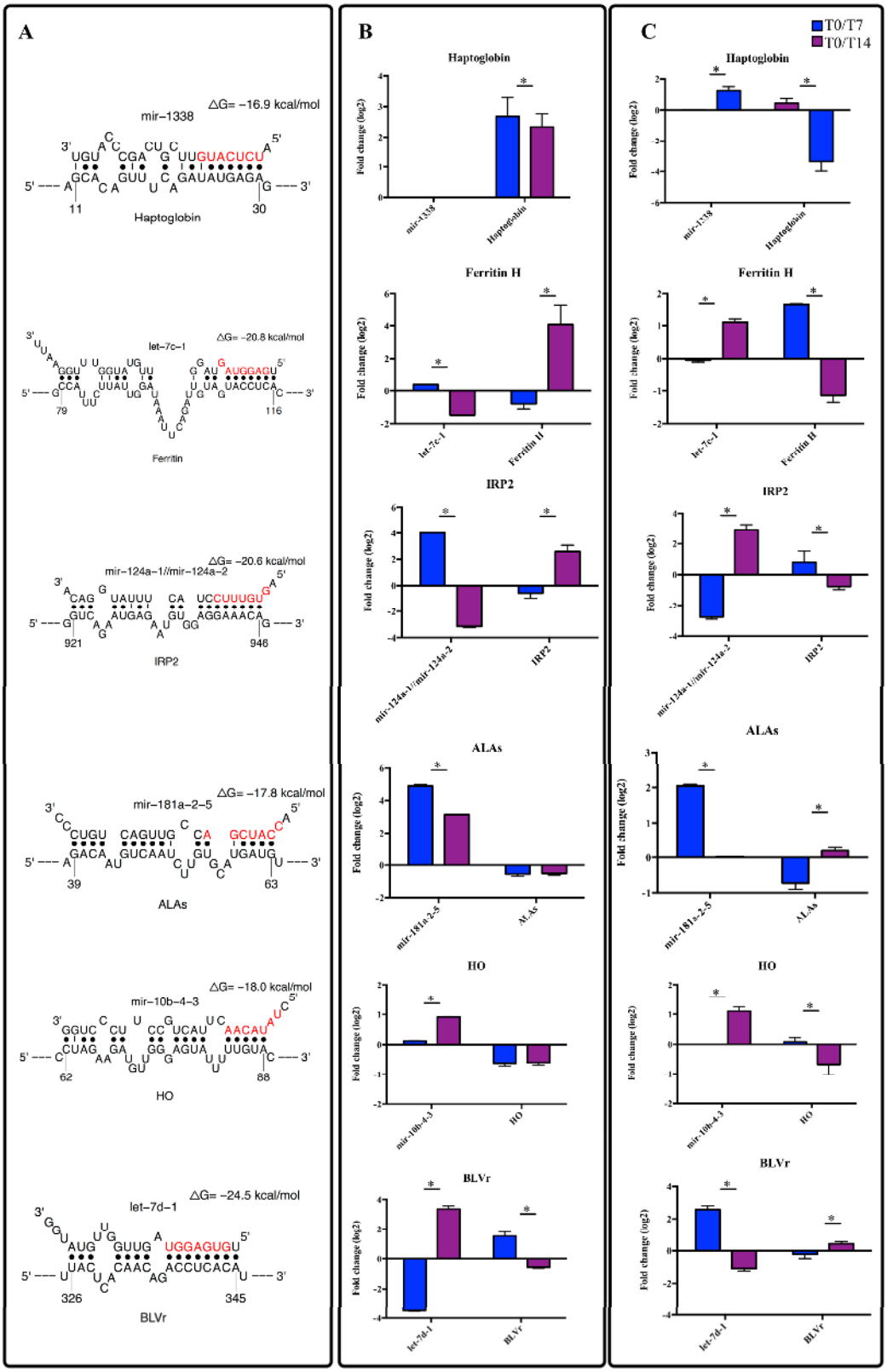
A
ΔG= −16.9 kcal/mol
mir−1338
Haptoglobin
ΔG= −20.8 kcal/mol
let−7c−1
Ferritin
ΔG= −20.6 kcal/mol
mir−124a−1/mir−124a−2
IRP2
ΔG= −17.8 kcal/mol
mir−181a−2−5
ALAs
ΔG= −18.0 kcal/mol
mir−10b−4−3
HO
ΔG= −24.5 kcal/mol
let−7d−1
BLVr
B
Haptoglobin
Ferritin H
IRP2
ALAs
HO
BLVr
Fold change (log2)
C
T0/T7
T0/T14
Haptoglobin
Ferritin H
IRP2
ALAs
HO
BLVr
Fold change (log2)

Figure 6

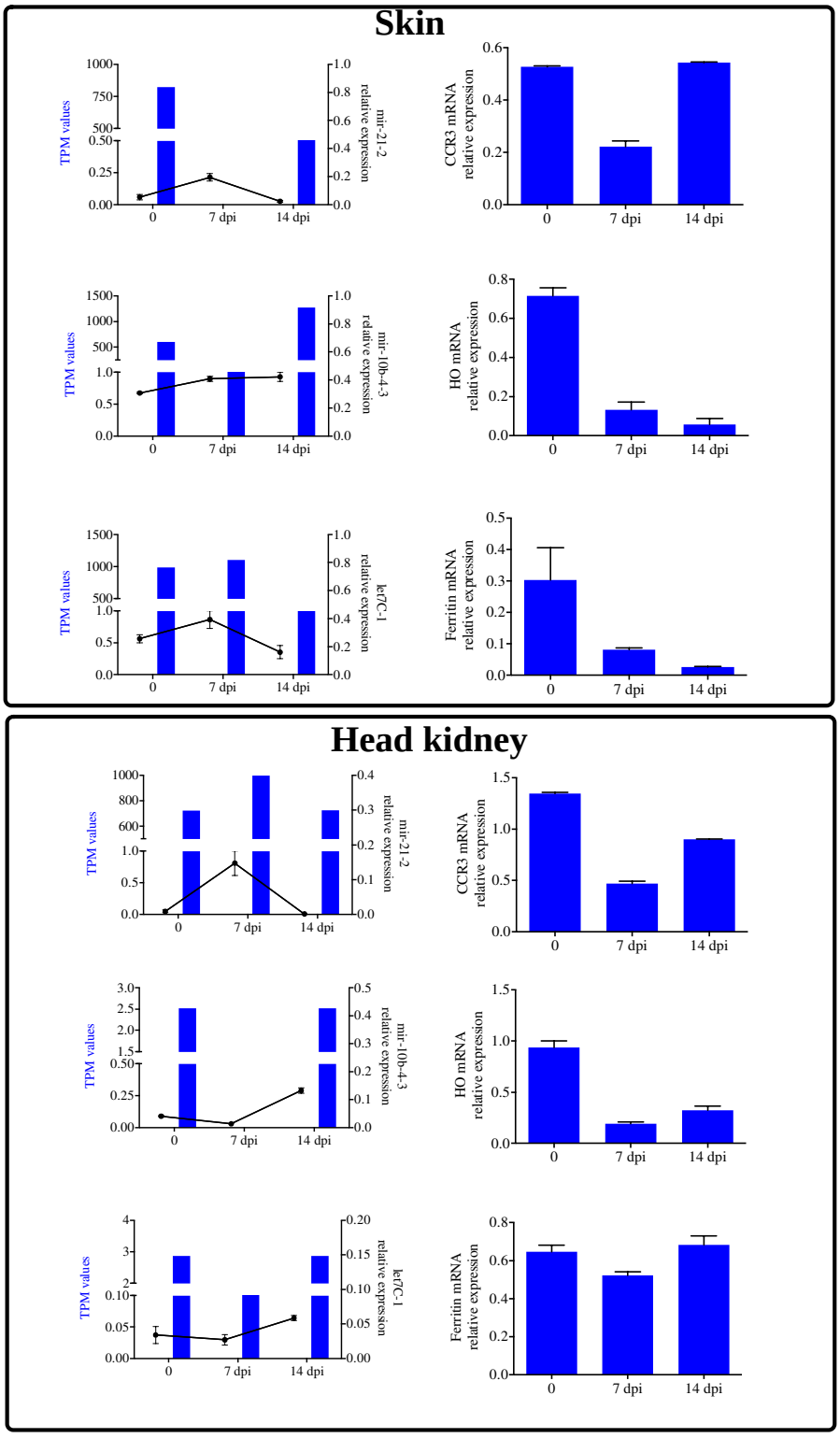
Skin
TPM values
mir-21-2
relative expression
CCR3 mRNA
relative expression
mir-10b-4-3
HO mRNA
let7C-1
Ferritin mRNA
0
7 dpi
14 dpi
Head kidney

Figure 7

Highlights

- A total of 1,718 miRNAs were annotated for skin and head kidney in Atlantic salmon infected with sea lice.
- The most abundant families identified were mir-10, mir-21, mir-30, mir-181 and let7.
- Infected-head kidney was primarily annotated with 1,404 miRNAs, meanwhile skin displayed 529 miRNAs.
- MiRNA target prediction revealed high modulation of immune-related genes and iron metabolism.